Estimating pelagic fish biomass in a tropical seascape using echosounding and baited stereo-videography

Running header (45 characters): Estimating biomass by combining acoustics and video

Tom B Letessier[1,2*], Roland Proud[3], Jessica J. Meeuwig[2], Martin J. Cox[4], Phil J. Hosegood[5], Andrew S. Brierley[3]

[1]Institute of Zoology, Zoological Society of London, Regent's Park, London NW1 4RY

[2]Marine Futures Lab, School of Biological Sciences and The Oceans Institute, The University of Western Australia, Crawley, Western Australia, Australia.

[3]Pelagic Ecology Research Group, Scottish Oceans Institute, Gatty Marine Laboratory, School of Biology, University of St-Andrews, KY16 8LB, United Kingdom.

[4]Australian Antarctic Division, Channel Highway, Kingston, TAS 7050, Australia

[5]School of Biological and Marine Sciences, University of Plymouth, Plymouth, United Kingdom

*Corresponding Author

Key words: Mid-water BRUVS, Marine Protected Areas, no-take, non-extractive.

Abstract

The pelagic ecosystem is the ocean's largest by volume and of major importance for food provision and carbon cycling. The high fish species diversity common in the tropics presents a major challenge for biomass estimation using fisheries acoustics, the traditional approach for evaluating mid-water biomass. Converting echo intensities to biomass density requires information on species identity and size, which are typically obtained by lethal means, and thus unsuitable in the portion of the ocean that is 'no take'. To improve conservation and ecosystem-based management, we present a procedure for determining fish biomass density, using data on species identity, relative abundance, and lengths obtained from stereo baited remote underwater video systems (stereo-BRUVS) to inform the scaling of echosounder survey data (at 38 kHz). We apply the procedure in the British Indian Ocean Territory marine protected area, using acoustic data from 3,025 km of survey transects and 546 BRUVS deployments recording relative abundance and size of 12,335 individual fish. Using a Generalised Additive Model of biomass density (GAM, adjR^2 = 0.61) we predict, on the basis of oceanographic conditions and bathymetry, that the top 200 m pelagic ecosystem in the Chagos Archipelago, some 118,324 km^2, held 3.84 (2.66, 5.62, 95% CI), 33.09 (23.41, 47.35) and 4.08 (3.1, 5.44) million tonnes of fish in November 2012, January 2015, and February 2016 respectively. Our non-extractive procedure yields ecologically-credible patterns in biomass across multiple temporal (hours and years) and spatial (meters and kilometres) scales, and marks an improvement on the use of echo intensity alone as a biomass proxy. High seasonal and interannual variability has implication for pelagic fish monitoring.

Highlights (no jargon, max 85 characters per bulletpoint)

- Lethal sampling for measuring fish biomass is inappropriate in no-take marine protected areas.
- We use baited cameras and echosounders to estimate fish biomass across an archipelago.
- Biomass differences between years have implication for monitoring and understanding ecosystem stressors.

Introduction

Food security, wildlife-conservation, and resource management require robust data on the abundance and biomass of species. In the marine realm, trawl and camera techniques for assessing demersal (seabed) fish populations are well established (Murphy and Jenkins 2010). Acoustic surveys using ship-mounted echosounders are often used as a component of fish population assessment because of the capability they have for near-instantaneous observations of almost the entire water-column (Simmonds and Maclennan 2005). Acoustic surveys are a kind of 'remote sensing' though, and require 'ground truth' data on species composition and size distribution to scale echo intensity data to fish abundance and/or biomass. For cases with a single species of interest (e.g. North Sea herring, Antarctic krill, tuna), biomass density can be determined accurately by combining acoustics with ground truth data from fishing, using for example trawling or longlining (Bertrand and Josse 2000; Fernandes and others 2002; Cox and others 2013). However, tools for monitoring highly-diverse, mixed species assemblages of fish are less well developed and assessments under such circumstances lack practical solutions, particularly in areas where fishing is prohibited or undesirable (Rosen and others 2013; Letessier and others 2017) such as no-take marine protected areas (MPAs).

For acoustic surveys, the principle of linearity holds that acoustic intensity from echoes is directly proportional to the numbers of fish insonified (Foote 1983). Acoustic target strength (TS, dB re 1 m^2) is a measure of the proportion of incident sound energy backscattered by an individual at a given frequency, and is a function of size, species, orientation and body density (Simmonds and Maclennan 2005). However, there can be considerable uncertainty in TS-to-fish length relationships when a diverse taxonomic assemblage of fish is present (Proud and others 2018). This is the case for many tropical systems, and uncertainty increases as the spatial and temporal scale of the survey increases, because the species number and size range typically increase, and so variability in sound scattering characteristics can be large (Holmin and others 2012; Irigoien and others 2014; Surette and others 2015). The need for high quality, independent data on species identifications and length is therefore critical for acoustic estimation of tropical pelagic fish assemblage biomass.

Baited remote underwater video systems (BRUVS) deliver data on fish species composition and size, and can – we propose – inform scaling of acoustic survey data. BRUVS are non-extractive and can be configured for use either on the seabed (Sherman and others 2018) or in the pelagic

(Letessier and others 2013; Bouchet and Meeuwig 2015). They can be used in situations where fishing is undesirable, prohibited (e.g. in no-take MPAs) or impossible (from vessels not able to trawl). Stereo-BRUVS yield fish species identity, relative abundance and length. However, the volume sampled by BRUVS is unknown, and varies depending upon on factors such as current velocity and fish swimming speed (Priede and Merrett 1996; Dunlop and others 2015). As a result, abundance and biomass measures from BRUVS are reported in relative terms only.

There is considerable impetus to develop new ways of sampling fish non-destructively, particularly for pelagic species. Many pelagic predatory fish such as tuna and sharks have experienced substantial declines over the last 65 years (Juan-Jordá and others 2011, Pacoureau and others 2021). Recent estimates suggest that 30% of the global ocean will have to be afforded strict no-take status to achieve effective protection (Sala and others 2018). Although vast oceanic regions are increasingly included within large no-take MPAs that may be large enough to cover the migration range of many pelagic predators (Boerder and others 2019), the effectiveness of such MPAs remains uncertain and is sometimes questioned (Sibert and others 2012; Dunne and others 2014). Key to solving this debate is a notable absence of effective methods for generating fishery-independent population time series (Letessier and others 2017).

In order to provide a quantitative method for generating biomass density of multispecies assemblages and biomass in complex, multispecies systems, we draw here on the recent advances in BRUVS technology (Letessier and others 2013; Bouchet and Meeuwig 2015) to provide the fish species and size data required to convert acoustic backscattering intensity data from echosounder surveys to fish biomass/abundance. Our observations were made inside the British Indian Ocean Territory MPA, presently the Indian Ocean's largest contiguous no-take area (640,000 km^2). The Indian Ocean remains one of the least regulated in terms of fishing (Hilborn and others 2020), with management challenges including unsustainable longline and purse-seine catches of yellowfin tuna (Rattle 2019), and high degrees of illegal fishing (Collins and others 2021a). BIOT contains diverse pelagic habitats over complex bathymetry (Sheppard and others 2012), many of which were targeted historically (Dunne and others 2014) prior to the formation of the MPA in 2010 (Koldewey and others 2010), with resulting declines in many mobile predators species (Ferretti and others 2018).

Our objectives here were 1) to develop a procedure to generate spatially resolved measures of fish biomass density, using acoustic observations and target strength estimates derived from fish species identification, relative abundance, and size data from BRUVS, and 2) to use geospatial

120 modelling to estimate spatial and temporal variability in biomass, thereby estimating the total
121 pelagic fish biomass across the archipelago, as a benchmark against which future change can be
122 evaluated. Our results have relevance for interpreting ecosystem stressors, and for ecosystem-
123 based management more broadly.
124

Material and Methods

The procedure for pelagic fish biomass density estimation presented here can be thought of as a recasting of the classic coupled acoustic observation and fishing approach used in fish stock assessment (acoustic-trawl surveys, Simmonds and Maclennan 2005), with the crucial difference that the identifications, relative abundances, and lengths of fish are derived from BRUVS, thus overcoming the need for extractive fishing. In the following description, we first give information on the specific field sampling material, design, and activities in the Chagos Archipelago, followed by a step-by-step description of the procedure to compute the biomass densities, which can be applied to any coupled acoustic-BRUVS observations.

Survey design and sampling activity

All acoustic and BRUVS observations were conducted inside the BIOT MPA, during three expeditions of approximately two to three weeks, in 2012 (22/11-08/12), 2015 (09/01-27/01), and 2016 (05/02-24/02). The expeditions overlapped with the peak historical November – February season for the purse-seine tuna fishery (Kaplan and others 2014), in order to get yearly snap-shots of the entire assemblage at the time of peak fishing activity. Observations were made between dawn and dusk (07:00 and 19:00 local time, Table 1) from the M/V Pacific Marlin. Our survey design reflected the primary objective of developing a sampling procedure using BRUVS and echosoundings, and the secondary and longer-term objective of capturing spatial and interannual variability, in order to establish a robust baseline for monitoring. Our design was therefore hierarchical, with paired acoustic and BRUVs sampling being clustered within six sites, partially replicated in-between years, and nested within broader archipelago-wide acoustic survey transects. The sites corresponded to habitats and features that were 1) broadly characteristic of the Chagos Archipelago region as a whole, and 2) hypothesised to be of relevance to pelagic ecology and fish distribution in general, such as seamounts (Yesson and others 2020) and coral reefs banks (Letessier and others 2019). The sites included shallow reefs (6 - 20 m seabed depth), shallow and deep seamounts (60 m and 1100 m summit depth), and deep basins (3,560 m, Table 1), and were in proximity to six nominal study sites: the Egmont atoll (Egm), the Sandes-Swart seamount (SaSw), the Marlin Mount (MaMo), on the Great Chagos Bank (GCB), the Peros Banhos and Salomon Atolls (PBSa), and north-west of the Archipelago (NW, Figure 1).

Acoustic surveys were conducted within each site using pole-mounted 38 and 120 kHz calibrated Simrad (Bergen, Norway) EK60 echosounders. While the BRUVS were deployed and centred on the habitat or feature sampled, the acoustic survey followed an expanding square, aiming to maximise the spatial and temporal overlap between the two sampling methods. Opportunistic acoustic data collection using the pole mount also occurred whilst deploying and recovering the BRUVS, and during other vessel activities. Data were collected opportunistically in all years, and were included in the analysis. Paired sampling at each site were nested within a large-scale acoustic transect across the Great Chagos Banks (in 2016), using 38, 120 and 200 kHz echosounders, fitted on a towed body (Figure 1) that, for logistic reasons, required higher speed passage (10 knots) than the pole mount could withstand (max 4 knots). The towed-body transect intersected the Great Chagos Banks twice, on a north-to-south and an east-to-west passage, and was designed to capture archipelago-wide patterns in fish biomass distribution.

The echosounders were calibrated using a standard sphere (Demer and others 2015) inside the MPA. The pulse length and ping rate were set at 1.024 ms and 0.5 Hz respectively. Acoustic data were processed using Echoview (v9, Myriax, Hobart, Australia) to remove background noise (Watkins and Brierley 2002) , ship movement noise, dropped pings, noise spikes, seabed and false-bottom echoes. The stereo-BRUVS were pre-calibrated using CAL software (SeaGIS PTY Ltd) following the procedure of Harvey and Shortis (1998).

We deployed drifting mid-water stereo-BRUVS, using rigs identical to those of Bouchet and Meeuwig (2015). Each were made up of a centre pole and a bait bar, with a bait canister containing 1 kg of crushed sardines, viewed by two stereo GoPros (Letessier and others 2015) each with a 4 degree inward convergent angle, located at c. 1.5 m from the cameras. Two strings of 5 rigs were deployed as a set. The strings were typically set approximately 1.5 nautical miles (nmi) apart, and left to drift freely for 2 hrs, approx. 1 nmi. The BRUVS were suspended at 10 meters depth, 200 m apart on each string, and were deployed across current. Each BRUVS was assigned a georeferenced position, defined by the mid-point between the entry and exit point of the deployment. Each site was typically sampled with between 5 and 8 string deployments over two days, per year (Table 1). BRUVS have been widely used to generate standardised estimates of fish species composition and size, and the strength and limitations are well established. The use of bait favours detection of predators and scavengers, and BRUVS are generally thought to capture a broader functional component of the assemblage, compared with fisheries sampling techniques such as trawls (e.g Cappo and others, 2004). The depth at which the rigs were

suspended (10 m), was a trade-off between the objective of surveying the mid-water fish assemblage in the epi-pelagic, and constraints imposed by having to support standardised sampling from different vessels of opportunity (e.g tenders, skiffs, dedicated research vessels etc).

Procedure for estimating fish biomass

The procedure was conducted for data across the six sites and comprises the following steps that are described in detail below: (1) processing of echosounder observations, including partitioning the acoustic data into the biological class of interest (such as 'large fish' or 'zooplankton') and removing noise; (2) generation of length and weight frequency-distributions using BRUVS data; (3) estimation of mean TS for the biological class of interest, and (4) conversion of echo intensity to biomass. In this instance, the biological class of interest was pelagic fish within 200m of the surface.

(1) Echosounder data were subset to include only observations made below a minimum sampling depth of 6 m (3 m pole depth plus c. 3 m acoustic near field; the towed body settled at a depth of 1 m during 10 knot transects) and above a maximum sampling depth of 800 m for seabed detections). Acoustic intensity of pelagic fish in the top 200 m was computed as the nautical-area scattering coefficient (NASC, Simmonds and Maclennan 2005), a linear measure of acoustic intensity summed over a depth range (see Maclennan and others 2002). The acoustic data were thresholded at -70 dB re 1 m^{-1} to remove weaker scatterers including zooplankton. Data recorded at 120 kHz were generally of lower quality than at 38 kHz, and were not used in this analysis.

(2) Upon recovery and subsequent video analysis, fish species identification, relative abundances, and length distributions were derived from the footage for each rig. Relative abundance per species per site was estimated as the maximum number of individuals observed at any one time during the 2 hr video recording for each rig (MaxN_{rig}), and then taking the maximum values of any single rig on the same string (MaxN_{string}). The use of Max*N* is considered a conservative measure of abundance (Bailey and others 2007), and is robust to change through time and space in the case of mid-water BRUVS (Letessier and others 2013). Max*N* remains the most commonly used metrics for analysing BRUVS videos

(Whitmarsh and others 2016) and there exists a wealth of knowledge concerning its strength and limitations (Schobernd and others 2014; Sherman and others 2018; Currey-Randall and others 2020). The use of MaxN ensures that an individual is only counted once, preventing the issue that arises when attempting to count unique individuals, which is difficult for most species (although possible for some, see Sherman and others 2018), or that arises from taking counts at intermitted time-intervals, which would favour species that linger at the bait. The use of MaxN_{string} as opposed to MaxN_{rig} effectively avoids recounts of individual fish that may occur in-between rigs on the same string.

(3) Fish fork lengths were recorded using EventMeasure software (SeaGIS 2008) at the time of MaxN_{rig} following standard stereo video measurement protocol (http://www.seagis.com.au/event.html). When a length measurement could not be made for a fish because, for example, it was out of range of the cameras or visually occluded, it was assigned by taking the first available length estimate from the following list of values: mean length of species for the site, mean length of species for archipelago, common length from FishBase, mean length of genus, mean length of family. We opted for this approach to ensure that all species were represented in the assemblage-wide biomass calculation. Since the objective was to provide lengths needed to parameterise conversion of acoustic intensity values into fish biomass, we opted to remove all lengths from elasmobranchs, since these do not have swimbladders and are therefore weak acoustic targets. In line with our objective to generate an assemblage-wide biomass measure using a NASC value that contained contributions from all fish species, we chose to convert the length to weights using a general conversion factor (equation [1]), taking the average conversion as reported by FishBase (Froese and Pauly 2015) for the species present, and scaled by MaxN_{string} abundance.

$$\text{Weight} = 0.012\ \mathrm{L_f}^{3.04} \qquad [1]$$

(4) Site-specific length distribution, of the entire species assemblage, were converted into acoustic TS values (Maclennan and others 2002). In the absence of any known species-specific conversion factors, length frequencies of all species were converted into TS, using the Foote (1987) generic fish TS-length equation and associated standard error [2].

$$\mathrm{TS_f} = 20\log_{10}\mathrm{L_f} - 67.5 \pm 2.3 \quad [2]$$

where L_f (cm) is the total fork length of the fish. The TS distribution and weight distributions were used to calculate mean echo energy per kg of fish (TS_{kg}), at each site. This acoustic conversion factor (Irigoien and others 2014) was estimated using equation [3].

$$\sigma_{\mathrm{kg}} = \overline{\sigma_{bs}}/\overline{\mathrm{w}} \quad [3]$$

where $\overline{\sigma_{bs}}$ and $\overline{\mathrm{w}}$ are the mean linear form of TS (backscattering cross-section; m^2) and mean weight (kg) respectively for each length distribution.

(5) Finally, the site-specific values of TS_{kg} were used to convert NASC values into fish biomass using equation [4].

$$b = \frac{NASC}{\sigma_{kg} \times 1{,}852^2 \times 4\pi} \times 1000 \quad [4]$$

where b (g m^{-2}) is fish biomass density and $'1{,}852^2 \times 4\pi'$ converts NASC to the area-backscattering coefficient (echo energy per m^2).

Predicting pelagic biomass throughout the Archipelago

To predict fish biomass across different seabed features and throughout the Chagos Archipelago, we built statistical geospatial models to predict likely values in unsampled regions. Observations from all sites were included within the same model to extract general trends across habitats; although it may have been possible to build more accurate predictions at the level of the habitat by using separate models for each site. In order to examine how our fish biomass density measure compared with a traditional measure of acoustic intensity, we built models predicting both NASC (m^2 nmi^{-2}) and fish biomass density (g m^2), as a function of bathymetric and oceanographic predictors (Table 2). On the grounds that pelagic biomass is expected to vary as a function of oceanographic and bathymetric characteristics, reflecting open ocean processes (Bouchet and

282 others, 2015; Irigoien and others, 2014) we expected the biomass density model to perform
283 better than the acoustic intensity model.
284 We used Generalised Additive Models (GAMs, Wood 2006), with a log link function and Gamma
285 error distribution and accounted for the inherent autocorrelation of acoustic intensity data using
286 a first-order autoregressive error structure (AR(1), Pinheiro and Bates 2000) fitted to each
287 transect. This approach is arguably a deviation from geostatistics, where kriging or the more
288 advanced class of log-Gaussian Cox processes can be applied (Teng and others 2017). Final
289 models derived from the full suite of candidate exploratory variables (Table 2) were selected
290 using stepwise forward selection based on the Akaike's information criterion (AIC, Akaike 1973).
291 When predicting biomass in areas that were not surveyed (out-of-sample predictions), we only
292 made predictions when conditions fell within the range of the explanatory variables (Table 2).
293
294

295 ## Result

296 ### Acoustic and BRUVS observations

297 A total of 3,025 km of acoustic survey transects were sampled within the archipelago, including
298 1,375 km covered by the pole-mounted system (in 2012, 2015 and 2016) and 1,650 km by the
299 towed body (2016). We observed a general two-layered vertical structuring in acoustic
300 backscatter, with one layer extending from the surface down to 200 m, and another from 300 m
301 to 600 m (Figure 2). These layers were present throughout the archipelago and have been
302 described in more detail elsewhere (Letessier and others 2016). Subsequent analysis focusses on
303 the epipelagic (0-200 m). Mean 38 kHz NASC per site, following thresholding, ranged between
304 171 (Marlin Mount) and 1,227 (Egmont) m^2 nmi^{-2} (Table 1, Figure 2). Assuming an assemblage of
305 fish of 20 cm length, this corresponds to a range of 55,776 to 400,414 individuals per km^2.
306 Five-hundred and forty-six BRUVS deployments yielded a total count of 12,335 individual fish
307 (sumMaxN_{rig}), representing 50 species and 27 families (Table 3), ranging in fork length between
308 1 and 356 cm (Figure 2). The greatest numbers of fish were observed off the Peros Banhos and
309 Salomon atolls (mean MaxN_{rig} 36.8 +/-6.5), whereas the least numbers of fish were recorded on
310 the Great Chagos Banks (mean MaxN_{rig} 2.25 +/-0.8, Table 3). Mean and maximum fish length
311 varied in between sites, with the largest individuals occurring in association with seamounts
312 (Sandes-Swartz and Marlin Mount). On an archipelago-wide scale, the total fish assemblage was
313 dominated by small scads (*Decapterus* spp, sumMaxN_{rig} =7520), spectacled filefish (*Cantherhines*
314 *fronticinctus,* sumMaxN_{rig} = 981), and juvenile bigeye trevally (*Caranx sexfasciatus,* sumMaxN_{rig} =
315 747, Table 3). The majority of species (n = 33) were of low overall abundance (sumMaxN_{rig} < 10).
316

317 ### Converting NASC to biomass

318 Acoustic intensity, captured with a sampling interval of 20 pings (80 m for the pole, 200 m for the
319 towed body), yielded a total of 10,025 individual NASC values for all three years/seasons
320 combined. Weak echoes (< -70 dB re 1 m^{-1}) attributed to zooplankton and excluded through
321 thresholding contributed only 4% of total NASC within the top 200 m. We opted to convert to
322 biomass only NASC values for which there were proximate BRUVS within a radial distance of the
323 site diameter, defined by the spread and centroid of the BRUVS cluster within a given site (Table
324 1, Figure 1). Data from outside the radial distance were excluded from further analyses. NASC
325 values within the radial distance of a BRUVS cluster centroid were all treated assuming the same

site-specific length/weight frequency distributions. This yielded a total of 7,201 individual biomass density values out of a total of 10,025 NASC values. The remaining 2,824 NASC values were not used further in this analysis.

Fish Biomass Predictions

The predictive capability of the acoustic intensity (NASC) GAM was low (adjR^2 = 0.36, Mean Absolute Error = 327.20 m^2 nmi^{-2}), compared with the biomass density model (adjR^2 = 0.61, Mean Absolute Error = 53.48 g m^{-2}, Table 4). Partial plots revealed biomass density increased in relation to proximity-to-reef (0.22 – 2.23 95% CI), sea-surface temperature (0.35 – 3.05 95% CI), and seabed depth (0.43 – 5.19 95% CI) (Figure 3). Biomass density appeared bimodal in relation to seabed depth, with elevated peaks in biomass occurring both at shallow (<500 m) and greater (>3500 m) seabed depths. GAM residuals were evenly distributed across the range of biomass density measurements (Figure 4).

Out-of-sample predictions were restricted to within 83 km from the reef and up to seabed depths of 3,560 m, the maximum distance from reef and seabed depth surveyed. This yielded predictions of fish biomass in unsampled areas within the MPA that had similar environmental characteristics to those of the sampled areas (Yates and others 2018), which amounted to 118,324 km^2, some 20% of the entire MPA. The top 200 m pelagic habitat (118,324 km^2) held, as predicted by GAMs, 3.84 (2.66 - 5.62 95% CI), 33.09 (23.41 - 47.35), and 4.08 (3.1 – 5.44) MT of fish, in 2012, 2015, and 2016, respectively (Figure 3).

The uncertainty in prediction varied across the archipelago, reducing towards the reef, reaching a minimum at 11.7 km from the reef edge (0.88 – 1.17 95% CI), and increasing out towards the open-ocean, reaching a maximum at 83 km (0.22 – 1.71 95% CI, Figure 3). Less sampling activity in sites with deeper seabed depths (Figure 1) meant that those predictions were associated with greater uncertainty (Figure 3).

Discussion

Recent assessment of global ocean sustainability has estimates that 21% and 28% no-take protection are required to maximise ecosystem and food provisioning benefits (Sala and others 2021). We have proposed and demonstrated a non-extractive (non-destructive), fisheries-independent procedure for generating pelagic fish biomass, suitable for use within such no-take areas. Our approach relies upon the recording of echoes, which is dependent on the inherent acoustic properties of mid-water animals, supplemented by optically derived information on individual fish, and thus combines the spatial-extensive coverage capability of underway acoustic surveys with the taxonomically resolved abundance and body size data from stereo-BRUVS. Geospatial models derived from our biomass measurements show improved predictability compared with acoustic intensity, thereby increasing the capacity to identify ecological patterns and understand processes within the protected sectors of the global ocean, currently growing at about 8% per year (Duarte and others 2020). As a consequence, our procedure greatly expands the area that can be monitored quantitatively in a sustainably managed ocean.

As with all survey methods, ours has strengths and weaknesses, some of which could be addressed with further sampling effort and research. Our sampling was by necessity limited to a sampling window of only two to three weeks per year. In addition, for several reasons, the portion of the fish assemblage sampled by the BRUVS overlap only in part with the portion insonified by the echosounders, leading to the following potential biases and areas of improvements:

Firstly, whereas the echosounder can sample continuously during vessel transit, BRUVS-based sampling is discrete in that BRUVS must be deployed and recovered each time, and were here limited to six different sites each of which represented different habitat types. The resolution could be improved by more incremental BRUVS-sampling.

Secondly, while considerable work has been done to understand how BRUVS compare with other fish sampling methods, active swimming toward the bait by mobile species means that BRUVS have an elevated probability of detecting predators and scavengers species (Watson and others 2005; Harvey and others 2007) compared with diver-based surveys. For high-order groups such as sharks BRUVS can therefore yield data comparable with scientific longline (Santana-Garcon and others 2014) and we would, as a consequence, expect that BRUVS are particularly robust for assessing change in populations of larger, predatory and often commercially important species,

such as tuna (*Thunnus* sp). The near-absence of yellowfin tuna (*Thunnus albacares*, the main target species of the historical fishery in BIOT, see Dunne and others, 2015) is therefore conspicuous, and could - speculatively - be related to the historically low levels of the Indian Ocean population (Rattle, 2019). However, for a given acoustic intensity, the propensity of BRUVS to attract predators is likely to yield a mean assemblage size that is on average larger than that of the assemblage insonified by the echosounder. As a consequence, we expect that – when converting acoustic intensity into kg using TS_{kg} for the entire assemblage– our method could potentially overestimate assemblage biomass density values.

Thirdly, as both our echosounder mounts (pole- or towed-body mounted) sampled at depth (> 3 m for the pole mount) the near-surface portion of the fish assemblage is likely not insonified. Surface aggregation is a major mechanism of trophic energy transfer in the tropics, whereby prey fish are eaten by predators such as tunas, sharks, cetaceans and seabirds (Maxwell and Morgan 2013). In the future, there may be considerable value in applying acoustic methods that are able to capture schools in the near-surface, for example, through horizontally facing echosounders, or side-scan sonar.

Fourthly, the placement at which we opted to fix the BRUVS from the surface (10 m) is likely to favour detection of species distributed toward the shallow end of the epipelagic. Although the bait is likely to attract fish from deeper than 10 m due to plume diffusion, the catchment is probably not going to extent to the full depth to which the acoustic intensity was computed (200 m), meaning that some species or demographic tranches will be missed. This may also include species which are not attracted to the bait. In sites where this is the case, one would expect TS values which are higher than expected from the abundances observed on the BRUVS It is notable than on the Great Chagos Bank the BRUVS fish assemblage appeared impoverished in both species richness and abundance (2.25 +/- 0.8 $MaxN_{rig}$) whereas NASC values were comparatively high (555.9 m^2 nmi^{-2} (482.9, 678.4)). With a shallow seabed of 50 meters, it is conceivable that the elevated TS is primarily driven by an assemblage of primarily benthic or benthopelagic composition, which the BRUVS would not have sampled equally. In the Chagos Archipelago, observations of acoustic scatterers within the top 200 m suggests a vertical partitioning of the assemblage. The nature of this partitioning, particularly how it relates to the shoaling of the thermocline (Currie and others 2013), could form the focus of further study using BRUVS deployed at variable depths within the epipelagic zone, which would also enable the correspondence between the BRUVS deployment depth and acoustic intensity to be optimized.

Fifthly, in the absence of published TS to length relationships for most species of fish, our approach assumes that the TS to length relationship of the species assemblage can be approximated by a generic function (Foote, 1987). Some pelagic species have very different swim bladder morphology (Kloser and others 1997), and gas inclusion in fish and zooplankton can contribute substantially to acoustic signal and TS (up to 95%, Foote 1980), so our procedure could be improved by identifying TS to length relationships on the basis of fish anatomy. The analysis could be further resolved by applying species-specific length to weight conversion, which are available for most taxa (Froese and Pauly 2015).

Sixthly, we opted to remove sharks (n = 271) from our BRUVS records, and focussed instead on the numerically dominant teleost component of the assemblage (> 99 %, sumMaxN_{rig}). We opted for this solution on the basis that sharks are poor acoustic targets, due to their lack of swim-bladders, and hence were unable to estimate shark biomass. A better solution to this limitation may arise from recent developments in split-beam multifrequency echosounders, where sharks are discriminated on the basis of their multifrequency spectrum (Korneliussen and others 2009). This approach could, in BIOT, yield shark abundances when estimates from extractive means are not possible (e.g Ferretti and others 2018).

We estimate that the archipelago ecosystems and surrounding oceanic habitat contained 33.09 (23.41, 47.35, 95% CI) million tonnes of pelagic fish, in the year 2015, at the time of survey. This is, to our knowledge, the first attempt at measuring pelagic fish biomass across the complex seascape of an archipelago, making comparison with estimates derived by other means difficult. Comparison is further complicated as most fisheries acoustic surveys tend to focus on assemblages that are either species poor or that are dominated by few species, such as in highly productive temperate or polar regions, or by deliberately targeting gear-restricted taxa (such as longline tuna) with well-defined acoustic properties and vertical distribution (i.e Bertrand and Josse 2000). Our estimates of individual biomass density spanned multiple orders of magnitude (0 – 2,200 g.m^{-2}), the upper range of which are consistent with those reported by underwater visual surveys, on the shallow reef of the Greater Chagos Bank (640 g. m^{-2}, MacNeil and others 2015), thereby lending confidence to our measurements. In addition, our decision to compute acoustic intensity (NASC) across the 0-200 m depth band appeared coherence with the fish assemblage observed on the BRUVS, since the bulk of the assemblage consisted of species living within the shallow scattering layer (< 200 m).

446 Consistent mean residual values across the range of predicted biomass levels gives credibility in
447 our spatial predictions, and can thus help interpret previous patterns in unidentified acoustic
448 intensity, as well as pinpointing knowledge gaps for future research. In the Chagos Archipelago,
449 increases in acoustic intensity near seamounts and atolls (Letessier and others 2016; Hosegood
450 and others 2019) translate here to an increase in fish biomass of 4.1 % (-0.65, 9.7, 95% CI) for
451 every 50 m decrease in seabed depth. Our observations of greater faunal variability associated
452 with increased distance from reefs and at greater seabed depth is typical of marine fauna in BIOT
453 (Perez Correa and others 2020) and elsewhere (Letessier and others 2019).
454 We observed that sea surface temperature, and thus oceanographic conditions more broadly,
455 have a direct impact on pelagic fish biomass. Understanding pelagic biomass variability at
456 multiple temporal (yearly and seasonally) scales is vital for understanding the ecosystem
457 resilience of the BIOT MPA, and has relevance for its management. Our survey in January 2015
458 occurred immediately prior to the 2015-2016 mass coral bleaching event (Head and others 2019)
459 which is believed to have led to a subsequent decline in demersal fish biomass (Benkwitt and
460 others 2019). It would be tempting, in a similar vein, to attribute the declines in pelagic fish
461 biomass that occurred between 2015 and 2016 to bleaching, were it not that pelagic biomass
462 levels were already low in November 2012. Given the importance of pelagic subsidies in
463 sustaining impoverished coral reef (Morais and Bellwood 2019), this variability has likely severe
464 consequences for the rebound potential of the demersal fish biomass, especially considering the
465 impoverished state the reefs are expected to be in after two back-to-back bleaching events.
466 We are unable to disentangle intra- and inter-annual variability from our three survey snap-shots,
467 and can only speculate as to the cause of this 10-fold biomass change (increasing between Nov
468 2012 and Jan 2015, and decreasing between Jan 2015 and Feb 2016). Oceanographic conditions
469 in the central tropical Indian Ocean are modulated by dynamic processes at annual timescales by
470 the Indian Ocean Dipole (Masumoto and others 2008), at seasonal timescales by the monsoon
471 (Schott and McCreary 2001), and with monthly periodicity by the Madden Julian Oscillation
472 (Resplandy and others 2009; Webber and others 2012) and equatorial Kelvin waves (Feng and
473 Meyers 2003). The resulting forcing causes the periodic eastward extension of the Seychelles
474 Chagos Thermocline Ridge into BIOT, which decreases surface temperature and raises
475 thermocline depth (Hermes and Reason 2008; Duvel and others 2009), promoting productivity
476 and influencing distributions and abundance of higher level predators (Lan and others 2013).
477 These processes, captured by the Indian Ocean Dipole index (Masumoto and others 2008), have

478 within BIOT been previously linked with interannual patterns in pelagic distribution of seabirds
479 (such as red boobies, Perez Correa and others, 2020), and are likely important in explaining the
480 10-fold interannual variability observed here. Furthermore, this suggests that a pelagic baseline
481 will need to be established across multiple years in order to understand the impact of ecosystem
482 stressors, to establish the effectiveness of MPA for pelagic species, and to guide MPA
483 management.
484 A non-compliant fishery remains active in BIOT and is thought to be highly seasonal throughout
485 the year, even though targeted reef sharks are themselves not seasonal (Collins and other
486 2021a). The seasonality of the fishers is thus more probably related to variability in pelagic fish,
487 and can thus more easily be anticipated (and thus intercepted by enforcement activity, Collins
488 and other 2021b) on the basis of pelagic and oceanographic processes. It is on this ground that
489 we propose that the open ocean ecosystems which includes areas previously targeted by the
490 historical fishing fleet (Dunn and others 2019) should be further prioritised by the BIOT
491 monitoring programme, in order to capture both seasonal and interannual variability.
492 Our procedure has yielded observations which help us interpret previous studies and are broadly
493 consistent with oceanographic processes. The method and results presented here are a first step
494 in generating a standardised time-series, and in determining the response of pelagic ecosystems
495 to different management regimes that increasingly includes no-take MPAs such as BIOT.
496 Critically, our estimation-related uncertainty is relatively small compared to inter-annual trends,
497 meaning that significant increases (or declines) in biomass can be spotted early. Although stereo
498 technology is increasingly used as an alternative to extractive methods (e.g for use in trawls with
499 open cod-ends, Garcia and others 2020) and in coupled fisheries-acoustics (Boldt and others
500 2018), this is to our knowledge the first attempt to parameterise echosounder observations using
501 baited videography. Our demonstration here was focussed on the mid-water and pelagic
502 ecosystem, the described procedure is equally applicable for communities living in association
503 with the seabed, or in deeper depth horizons, such as the mesopelagic (Irigoien and others 2014).
504 Given the recent establishment of BRUVS as a pelagic monitoring standard across the UK's
505 Overseas Territories 'Blue Belt' of protected ocean (Meeuwig and others 2021), and the already
506 firmly intrenched status of fisheries acoustics as a staple of pelagic monitoring (Proud and others
507 2017), our procedure - whereby a harmonious merging of the two is achieved by collecting
508 acoustic data en-route with intermittent stereo-BRUVS at regular intervals - is a powerful tool
509 yielding both the scale and resolution required for basin-wide fish biomass surveys.

Acknowledgement

This research was conducted under permits and support granted by the British Indian Ocean Territory's Administration and the Foreign and Commonwealth Office of the United Kingdom, and under ethics approval and permit RA/3/100/1166 and RA/3/100/1386 from the Animal Ethics Committee of the University of Western Australia, following guidelines under the Animal Welfare Act 2002 (WA) and the Australian Code for the Care and Use of Animals for Scientific Purposes. This paper is an output of the Bertarelli Programme in Marine Science, and we are grateful for the Bertarelli Foundation's support. We thank Christopher D. H. Thompson and Marjorie Cattaneo Fernandes for contributions to the BRUVS deployments and video analysis. We are grateful to Marine Science Scotland for lending us the towed body for the 2016 expedition, and in particular Eric Armstrong and Phil Copland for towed body preparation and shipping. Finally, for excellent assistance, fond memories and friendship, we thank the Master, Chief and crew of the support vessel.

Figures

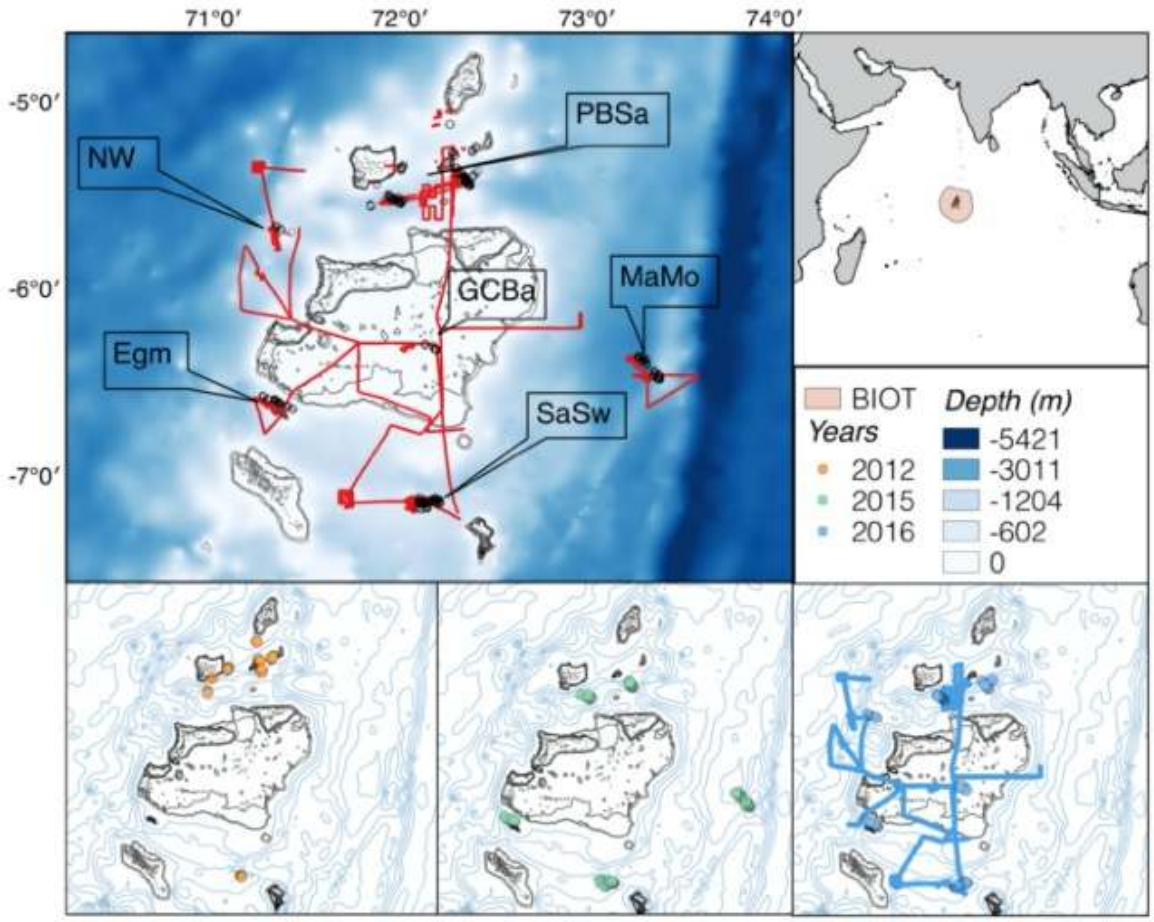

Figure 1 Coupled acoustic (red lines) and mid-water baited remote underwater video systems (open black circles) sampling activity within the British Indian Ocean Territory fisheries exclusion zone (inset), in November 2012, January 2015 and February 2016 (bottom panels, in chronological order, showing 500 m isobaths). Labels denote sampling sites, defined by BRUVS clusters, at North Western Station (NW), Peros-Banhos and Salomon atolls (PBSa), Great Chagos Banks (GCB), Marline Mount (MaMo), Egmont atoll (Egm), and Sandes Swart seamount (SaSw).

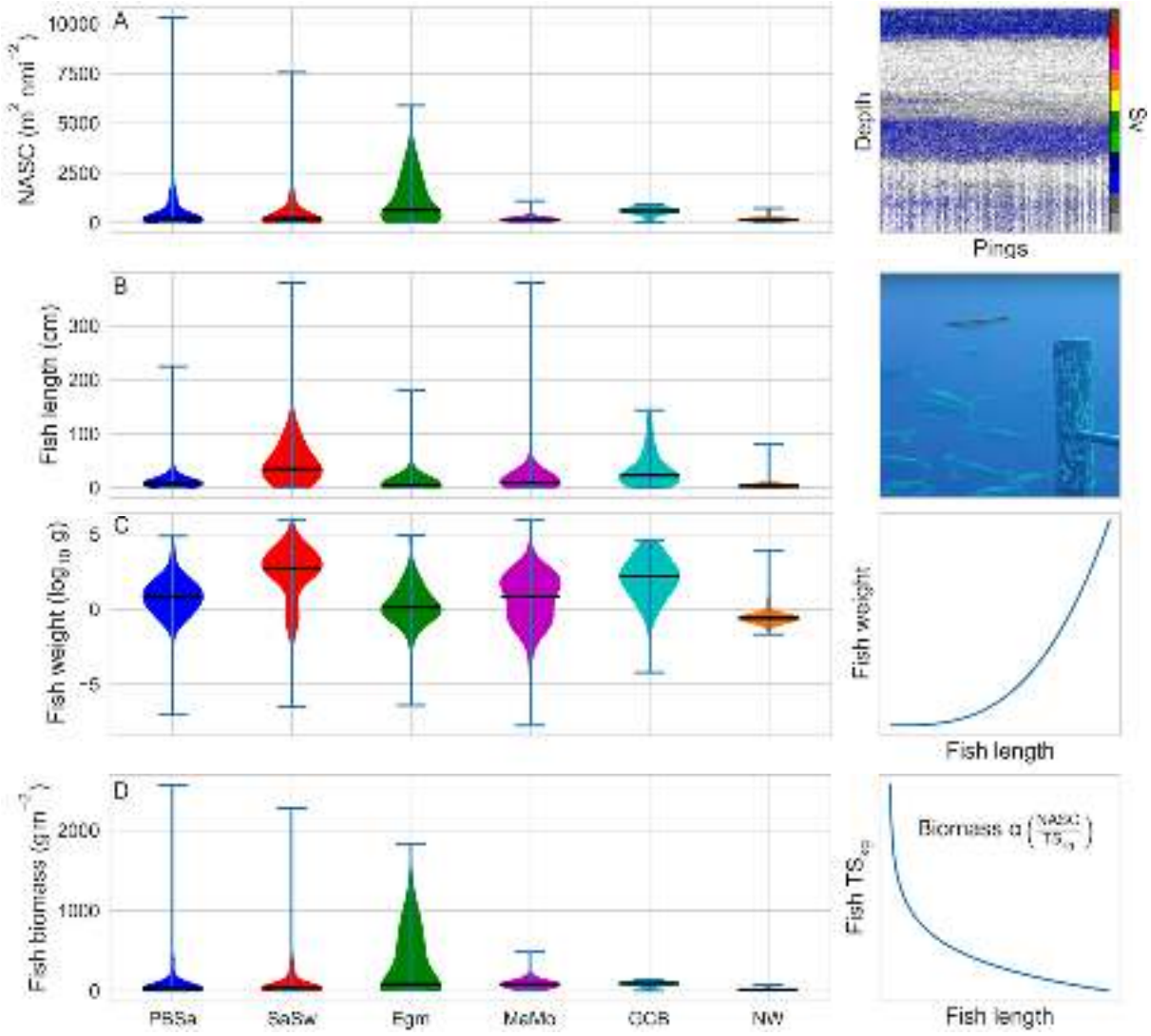

535

536 **Figure 2** Steps required for converting echo intensity to biomass using baited camera
537 measurements: A) Acoustic intensity distribution (left pane) and typical echogram (right pane; n
538 pings = 200; depth range = 800 m), computed as nautical-area scattering coefficient (NASC, m^2
539 nmi^{-2}), averaged into 20 ping by 200 m depth cells. B) Fish fork length distribution (left pane),
540 derived from stereo baited remote underwater videos systems (illustrated by a typical frame,
541 right pane). C) Weight distributions calculated from weight-length relationship (right pane). D)
542 Fish biomass distribution (left pane), calculated by converting NASC observations to biomass
543 using acoustic conversion factor, TS_{kg} (right pane).
544

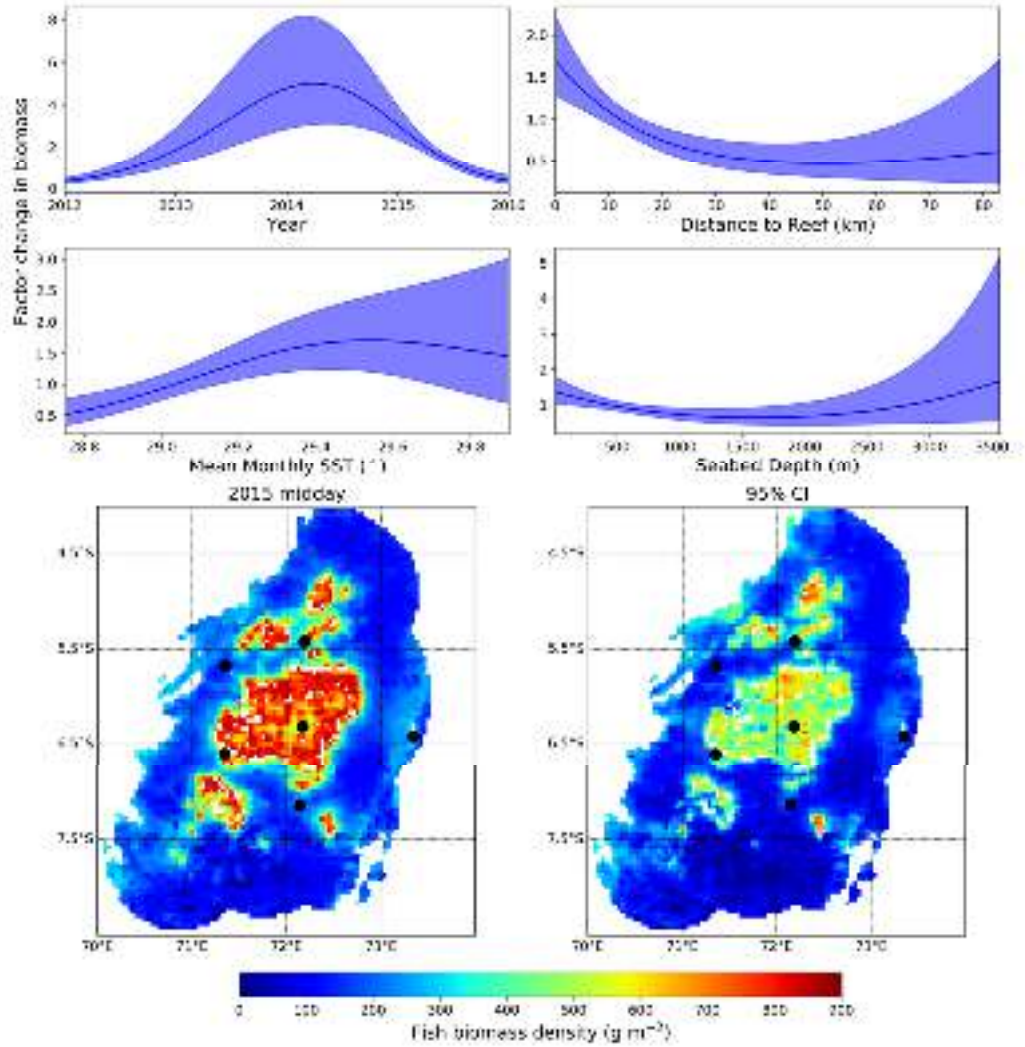

Figure 3 Estimating pelagic fish biomass density in the Chagos Archipelago. Generalised Additive Model partial plots (top two panel rows), predictions of pelagic fish biomass density (for the year 2015, at midday, bottom left panel), and confidence interval (95% CI, bottom right panel) across the Chagos Archipelago. Centroids of BRUVS cluster sites are marked by black spots. Mean fish biomass density is 279.68 (197.87, 400.15) g m^{-2}, yielding 33.09 (23.41, 47.35) million tonnes of fish for the year 2015.

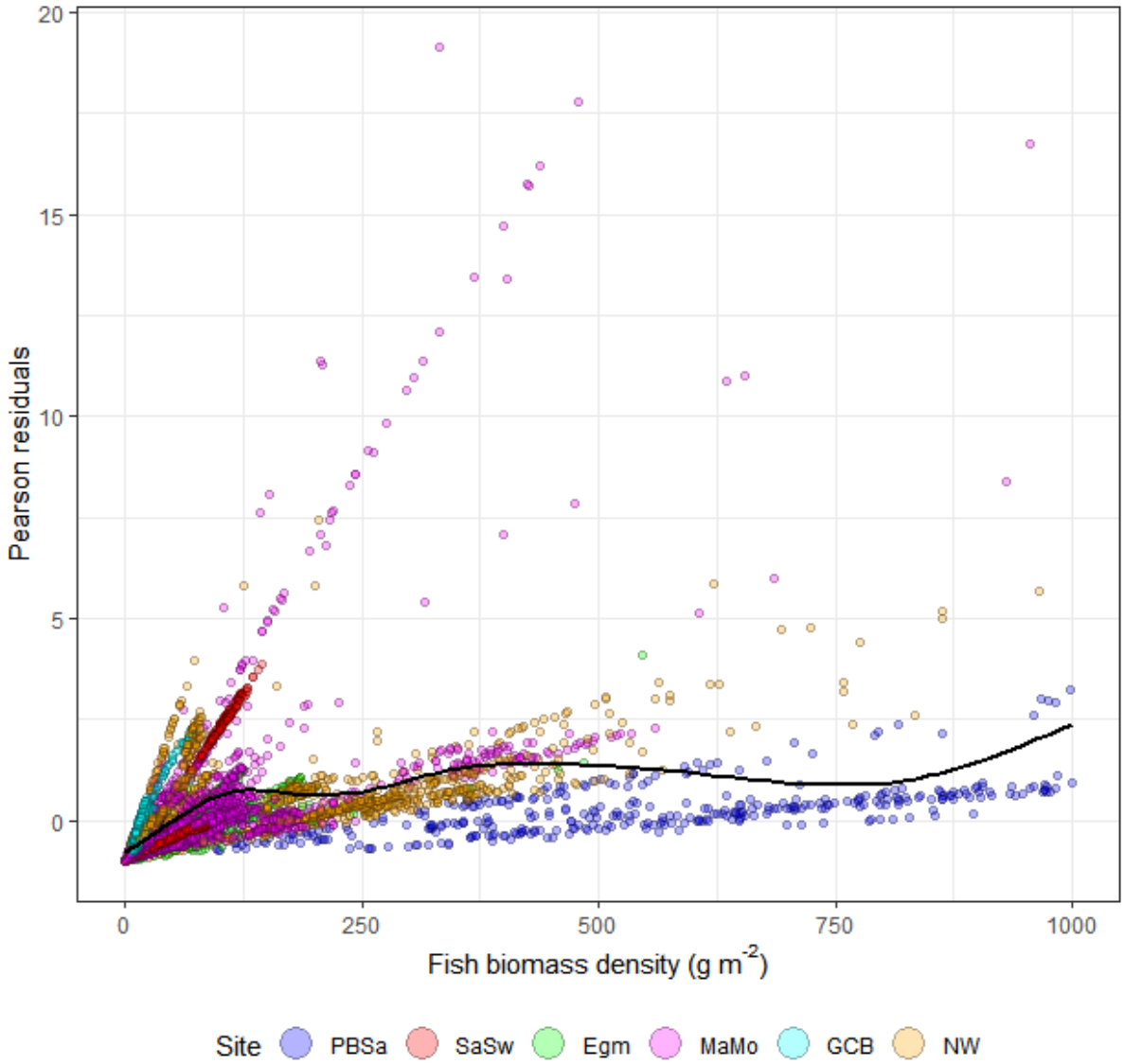

Figure 4 Smooth functions (black line) showing mean Pearson residuals from the fish biomass density GAM predictions, colour coded for site.

Tables

Table 1 Sampling sites and summary statistics of acoustic and stereo-BRUVS observations of pelagic fish abundance (Mean MaxN_{rig})

Site	Lat	Lon	Year sampled	Mean NASC (m^2 nmi^{-2}) [lower quartile, upper quartile]	Survey tracks (km)	Site area (radial distance, km)	Number of BRUVS deployments	Mean MaxN_{rig} (s.e)	Number of BRUVS deployments
Sandes-Swart Seamount (SaSw)	-7.1	72.1	2012, 2015, 2016	527.3 (113.9, 791)	463	7.6	134	9.4 (1.8)	134

Perhos Banhos and Salmon atoll (PBSa)	-5.4	72.2	2012, 2015, 2016	364.9 (76.1, 315.6)	512	41.2	246	36.8 (6.5)	246
Northwest station (NWst)	-5.7	71.4	2016	187 (124.8, 202.3)	112	7.4	10	4 (0.7)	10
Great Chagos Banks (GCB)	-6.3	72.2	2016	555.9 (482.9, 678.4)	29	4.5	20	2.25 (0.8)	20
Egmont (Egm)	-6.6	71.3	2015	1227.4 (250.4, 1988.3)	168	10.3	56	18.3 (6.4)	56
Marlin Mount (MaMo)	-6.4	73.3	2015	171.1 (92.7, 164.9)	238	9.9	80	11.2 (2.7)	80

560

561 **Table 2** Predictors of pelagic fish biomass and sources.

Predictor and unit	Resolution	Range	Source	Reference and rational
Seabed depth (m)	80 m	5 - 3,560	Echosounder and GEBCO (www.gebco.net)	(Boersch-Supan and others 2017)
Distance to reef (km)	NA	0-83	Millennium Coral Reef Mapping Project (http://imars.marine.usf.edu/millennium-coral).	(Letessier and others 2016)
Chla (mg m^{-3})	4 km, Monthly means	0-0.25	https://oceancolor.gsfc.nasa.gov/data/aqua/	(Proud and others 2017)
SST (°)	4 km, Monthly means	28.76-29.91	https://oceancolor.gsfc.nasa.gov/data/aqua/	(Boersch-Supan and others 2017)
SST s.d. (°)		0.3-0.8	https://oceancolor.gsfc.nasa.gov/data/aqua/	(Boersch-Supan and others 2017)
Hours	NA	8 am-7pm		(Brierley 2014)
Year	NA	2012, 2015, 2016		(Curnick and others 2020)

562

563 **Table 3** Fish families and species and their abundance (MaxN_{rig}), as recorded by mid-water
564 BRUVS, in the British Indian Ocean Territory at each site: North Western Station (NW), Peros-
565 Banhos and Salomon atolls (PBSa), Great Chagos Banks (GCB), Marlin Mount (MaMo), Egmont
566 atoll (Egm), and Sandes-Swart seamount (SaSw).

	Egm	GCB	MaMo	NW	PBSa	SaSw	sumMaxN_{rig}
Acanthuridae					1		1
Naso sp					1		1
Apogonidae						1	1
Ostorhinchus holotaenia						1	1
Balistidae	3				3	4	10
Abalistes stellatus					2		2
Canthidermis maculata	3				1	4	8
Belonidae				1			1
Ablennes hians				1			1
Blenniidae	13	1		1	22	15	52
Aspidontus dussumieri	12	1		1	14	14	42
Aspidontus taeniatus	1				4	1	6
Plagiotremus tapeinosoma					4		4
Carangidae	873	31	445	23	7360	621	9353
Carangidae sp					22	4	26
Caranx sexfasciatus	43	8	3	18	658	17	747

Decapterus macarellus					751	3	754
Decapterus sp	822	23	438	5	5909	323	7520
Elagatis bipinnulata	8				16	272	296
Naucrates ductor			4		1	2	7
Scomberoides sp					3		3
Carcharhinidae	1		1		28	238	268
Carcharhinidae sp					1	1	2
Carcharhinus albimarginatus						151	151
Carcharhinus amblyrhynchos					3	30	33
Carcharhinus falciformis	1				23	56	80
Carcharhinus longimanus			1				1
Galeocerdo cuvier					1		1
Chaetodontidae					1		1
Heniochus sp					1		1
Clupeidae	32						32
Clupeidae sp	32						32
Coryphaenidae	2		17	1	18	4	42
Coryphaena hippurus	2		17	1	18	4	42
Echeneidae		8	1		4	3	16
Echeneis naucrates					1	1	2
Remora albescens					1		1
Remora remora		8	1		2	2	13
Fistulariidae	12	1		2	12	8	35
Fistularia commersonii	7	1		2	12	8	30
Fistularia petimba	5						5
Istiophoridae			2		3	4	9
Istiompax indica			2		1	3	6
Istiophorus platypterus					2		2
Makaira nigricans						1	1
Lamnidae					2		2
Isurus oxyrinchus					2		2
Lobotidae	2						2
Lobotes surinamensis	2						2
Lutjanidae	2				30		32
Lutjanus bengalensis	2				30		32
Molidae			1				1
Mola mola			1				1
Monacanthidae	32	1	1	11	974	6	1025
Aluterus monoceros			1				1
Aluterus scriptus					41	1	42
Cantherhines fronticinctus	32	1		11	932	5	981
Pseudalutarius nasicornis					1		1
Mullidae	29		1		195		225
Parupeneus barberinus					2		2
Parupeneus macronemus	29		1		193		223
Myliobatidae					1		1

Mobula japanica					1		1
Nomeidae	26		418	1	121	96	662
Psenes cyanophrys	26		418	1	121	96	662
Pomacentridae					6		6
Pomacentrus caeruleus					6		6
Priacanthidae					2		2
Priacanthus blochii					2		2
Rhincodontidae					1		1
Rhincodon typus					1		1
Scombridae		3	4		272	261	540
Acanthocybium solandri		3	2		5	18	28
Euthynnus affinis			2		179	41	222
Scombridae sp						1	1
Thunnus albacares					1		1
Thunnus obesus						5	5
Thunnus orientalis					87		87
Thunnus tonggol						196	196
Sphyraenidae			4		1	7	12
Sphyraena barracuda			4			4	8
Sphyraena jello					1		1
Sphyraena sp						3	3
Sphyrnidae						2	2
Sphyrna lewini						2	2
Grand Total	1027	45	895	40	9058	1270	12335

567
568

569 **Table 4** Description of final Generalised Additive Mixed Models for acoustic intensity (NASC) and
570 fish biomass density.

		Fish NASC (m^2 nmi^{-2})	Fish biomass (g m^{-2})
Parametric terms (s.e.)	Intercept	8.08*** (0.15)	5.58*** (0.15)
	Hour	-0.15*** (0.01)	-0.11*** (0.01)
Smooth terms (F)	Year	1.97*** (184.98)	2.00*** (294.82)
	SST	1.97*** (14.53)	1.97*** (32.93)
	$dist_{reef}$	1.93*** (44.10)	1.97*** (34.30)
	seabed	1.96*** (10.11)	1.97*** (20.72)
Model evaluation	AR(1) correlation coefficient (95% CI)	0.77 (0.75, 0.78)	0.77 (0.75,0.78)
	AIC	26037	16199
	$adjR^2$	0.36	0.61
	cor	0.6	0.78
	MAE	327.20	53.48
	n	10,025	7,201
Model predictions (95% CI)			
Areal mean (hour = 12)	2012	79.69 (55.87,114.42) m^2 nmi^{-2}	32.45 (22.46, 47.53) g m^{-2}
	2015	731 (527.07,1021.94) m^2 nmi^{-2}	279.68 (197.87, 400.15) g m^{-2}
	2016	540.52 (431.15, 682.24) m^2 nmi^{-2}	34.52 (26.16, 46) g m^{-2}
Total (hour = 12)	2012	0.22e6 (0.15e6, 0.31e6) m^2	3.84 (2.66, 5.62) Mt
	2015	2e6 (1.45e6, 2.81e6) m^2	33.09 (23.41, 47.35) Mt
	2016	1.48e6 (1.18e6, 1.87e6) m^2	4.08 (3.1, 5.44) Mt

571

572

References

Akaike, H. 1973. Information Theory and an extension of the maximum likelihood B.N. Petrov and F. Cs'aki [eds.]. International Symposium on Information Theory 267–281.

Bailey, D. M., King, N. J., and Priede, I. G. 2007. Cameras and carcasses: historical and current methods for using artificial food falls to study deep-water animals. Marine Ecology Progress Series 350: 179–191. doi:10.3354/meps07187

Benkwitt, C. E., Wilson, S. K., and Graham, N. A. J. (2019). Seabird nutrient subsidies alter patterns of algal abundance and fish biomass on coral reefs following a bleaching event. Global Change Biology, *20*(8), 2459–14. http://doi.org/10.1111/gcb.14643

Bertrand, A., and Josse E. 2000. Acoustic estimation of longline tuna abundance. ICES Journal of Marine Science 57: 919–926. doi:10.1006/jmsc.2000.0579

Boerder, K., Schiller, L., and Worm B. 2019. Not all who wander are lost: Improving spatial protection for large pelagic fishes. Marine Policy 105: 80–90. doi:10.1016/j.marpol.2019.04.013

Boersch-Supan, P. H., Rogers, A. D, and Brierley, A. S. 2017. The distribution of pelagic sound scattering layers across the southwest Indian Ocean. Deep Sea Research Part II: Topical Studies in Oceanography 136: 108–121. doi:10.1016/j.dsr2.2015.06.023

Boldt, J. L., Williams, K., Rooper, C. N., Towler, R. H., and Gauthier, S. (2018). Development of stereo camera methodologies to improve pelagic fish biomass estimates and inform ecosystem management in marine waters. Fisheries Research, 198, 66–77. http://doi.org/10.1016/j.fishres.2017.10.013

Bouchet, P. J., and Meeuwig, J. J . 2015. Drifting baited stereo-videography: a novel sampling tool for surveying pelagic wildlife in offshore marine reserves. Ecosphere 6: art137. doi:10.1890/ES14-00380.2

Bouchet, P. J., Meeuwig, J. J., Salgado Kent, C. P., Letessier, T. B., and Jenner, C. K. (2015). Topographic determinants of mobile vertebrate predator hotspots: current knowledge and future directions. *Biological Reviews*, *90*(3), 699–728. http://doi.org/10.1111/j.1467-2979.2012.00483.x

Brierley, A. S. 2014. Diel vertical migration. Current Biology 24: R1074–6. doi:10.1016/j.cub.2014.08.054

Collins, C., Nuno, A., Benaragama, A., Broderick, A. C., Wijesundara, I., Wijetunge, D., and Letessier, T. B. (2021a). Ocean-scale footprint of a highly mobile fishing fleet: social-ecological drivers of fleet behaviour and evidence of illegal fishing. People and Nature.

Collins, C., Nuno, A., Broderick, A. C., Curnick, D. J., de Vos, A., Franklin, T., and others (2021b). Understanding persistent non-compliance in a remote, large scale marine protected area. Frontiers in Marine Science.

Cox, M. J., Letessier, T. B., and Brierley, A. S. 2013. Zooplankton and micronekton biovolume at the Mid-Atlantic Ridge and Charlie-Gibbs Fracture Zone estimated by multi-frequency acoustic survey. Deep Sea Research Part II: Topical Studies in Oceanography 98: 269–278. doi:10.1016/j.dsr2.2013.07.020

Curnick, D. J., Collen, B., Koldewey, H. K., Jones, K. E., Kemp, K. M., and Ferretti F., 2020. Interactions between a large marine protected area, pelagic tuna and associated fisheries. Frontiers Marine Science doi:10.3389/fmars.2020.00318

616 Currey-Randall LM, Cappo M, Simpfendorfer CA, Farabaugh NF, Heupel MR. 2020. Optimal soak
617 times for Baited Remote Underwater Video Station surveys of reef-associated
618 elasmobranchs. Januchowski-Hartley FA, editor. PloS one 15:e0231688–20.

619 Currie, J. C., Lengaigne, M., Vialard, J., Kaplan, D. M., Aumont, O., Naqvi, S. W. A., and Maury, O.
620 (2013). Indian Ocean Dipole and El Niño/Southern Oscillation impacts on regional
621 chlorophyll anomalies in the Indian Ocean. Biogeosciences, 10(10), 6677–6698.
622 http://doi.org/10.5194/bg-10-6677-2013
623 Dunn, N., and Curnick, D. (2019). Using historical fisheries data to predict tuna distribution
624 within the British Indian Ocean Territory Marine Protected Area, and implications for its
625 management. Aquatic Conservation: Marine and Freshwater Ecosystems, 101, 215–14.
626 http://doi.org/10.1002/aqc.3204
627 Demer, D., Berger, L., Bernasconi, M., Bethke, E., Boswell, K. M., Chu, D., and others (2015).
628 Calibration of acoustic instruments. ICES Cooperative Research Report, 326, 133.
629 Duarte, C. M., Agusti, S., Barbier, E., and others. 2020. Rebuilding marine life. Nature 1–13.
630 doi:10.1038/s41586-020-2146-7
631 Dunlop, K. M., Ruxton, G. D., Scott, E.M., and Bailey, D. M., 2015. Absolute abundance
632 estimates from shallow water baited underwater camera surveys; a stochastic modelling
633 approach tested against field data. Journal of Experimental Marine Biology and Ecology
634 472: 126–134. doi:10.1016/j.jembe.2015.07.010
635 Dunne, R. P., Polunin, N. V. C., Sand, P. H., and Johnson, M. L . 2014. The Creation of the Chagos
636 Marine Protected Area: A Fisheries Perspective. Marine Managed Areas and Fisheries 69:
637 79–127. doi:10.1016/B978-0-12-800214-8.00003-7

638 Duvel, J.P., Bouruet-Aubertot, P., Ward, B., and others. 2009. Cirene: Air—Sea Interactions in
639 the Seychelles—Chagos Thermocline Ridge Region. Bulletin of the American Meteorological
640 Society 90: 45–62. doi:10.1175/2008BAMS2499.1
641 Fassler, S. M. M., Gorska, N., Ona, E., and Fernandes, P. G. (2008). Differences in swimbladder
642 volume between Baltic and Norwegian spring-spawning herring: Consequences for mean
643 target strength. Fisheries Research, 92(2-3), 314–321.
644 http://doi.org/10.1016/j.fishres.2008.01.013
645 Feng, M., and Meyers, G. 2003. Interannual variability in the tropical Indian Ocean: a two-year
646 time-scale of Indian Ocean Dipole. Deep Sea Research Part II: Topical Studies in
647 Oceanography 50: 2263–2284. doi:10.1016/S0967-0645(03)00056-0
648 Fernandes, P. G., Gerlotto, F., Holliday, D., Nakken, O., and Simmonds, E. J. 2002. Acoustic
649 applications in fisheries science: the ICES contribution. ICES Marine Science Symposia 483–
650 492.
651 Ferretti, F., Curnick, D., Romanov, E. V., and Block, B. A. 2018. Shark baselines and the
652 conservation role of remote coral reef ecosystems. Science Advances 4:eaaq0333
653 Foote, K. G. 1980. Importance of the swimbladder in acoustic scattering by fish: a comparison of
654 gadoid and mackerel target strengths. Journal of the Acoustical Society of America, 67,
655 2084-2089.
656 Foote, K. G. 1983. Linearity of fisheries acoustics, with addition theorems. Journal of the
657 Acoustic Society of America 73: 1932–1940. doi:10.1121/1.389583
658 Foote, K. G. 1987. Fish Target Strengths for Use in Echo Integrator Surveys. Journal of the
659 Acoustic Society of America 82: 981–987.
660 Froese, R., and Pauly, D. 2015. FishBase. World Wide Web electronic publication.

661 Garcia, R., Prados, R., Quintana, J., Tempelaar, A., Gracias, N., Rosen, S., and others (2020).
662 Automatic segmentation of fish using deep learning with application to fish size
663 measurement. ICES Journal of Marine Science, 77(4), 1354–1366.
664 http://doi.org/10.1093/icesjms/fsz186
665 Harvey, E.S. and Shortis, M.R. (1998) Calibration stability of an underwater ste- reo-video
666 system: implications for measurement accuracy and precision. Marine Technology Society
667 Journal, 32, 3–17.
668 Harvey, E. S., Cappo, M., Butler, J., Hall, N., and Kendrick, G. 2007. Bait attraction affects the
669 performance of remote underwater video stations in assessment of demersal fish
670 community structure. Marine Ecology Progress Series 350: 245–254.
671 doi:10.3354/meps07192
672 Head, C. E. I., Bayley, D. T. I., Rowlands, G., Roche, R. C., Tickler, D. M., Rogers, A. D., and others.
673 (2019). Coral bleaching impacts from back-to-back 2015–2016 thermal anomalies in the
674 remote central Indian Ocean. Coral Reefs, 1–14. http://doi.org/10.1007/s00338-019-01821-
675 9
676 Hermes, J. C., and Reason, C. J. C. 2008. Annual cycle of the South Indian Ocean (Seychelles-
677 Chagos) thermocline ridge in a regional ocean model. Journal of Geophysical Research 113:
678 2305. doi:10.1029/2007JC004363
679 Hilborn, R., Amoroso, R. O., Anderson, C. M., and others. 2020. Effective fisheries management
680 instrumental in improving fish stock status. Proceedings of the National Academy of
681 Sciences 1–7. doi:10.1073/pnas.1909726116
682 Holmin, A. J., Handegard, N. O., Korneliussen, R. J., and Tjøstheim, D. 2012. Simulations of
683 multi-beam sonar echos from schooling individual fish in a quiet environment. Journal
684 Acoustic Society America 132: 3720–3734. doi:10.1121/1.4763981

685 Hosegood, P. J., Nimmo-Smith, W. A. M., Proud, R., Adams, K. and Brierley, A. S. 2019. Internal
686 lee waves and baroclinic bores over a tropical seamount shark “hot-spot.” Progress in
687 Oceanography 172: 34–50. doi:10.1016/j.pocean.2019.01.010
688 Irigoien, X., Klevjer, T. A., Røstad, A., and others. 2014. Large mesopelagic fishes biomass and
689 trophic efficiency in the open ocean. Nature Communications 5: 1–10.
690 doi:10.1038/ncomms4271
691 Kloser, R. J., Williams, A., and Koslow, J. A. (1997). Problems with acoustic target strength
692 measurements of a deepwater fish, orange roughy (*Hoplostethus atlanticus*, Collett). Ices
693 Journal of Marine Science, 54, 60–71.
694 Kaplan, D. M., Chassot, E., Amande, J. M., Dueri, S. , Demarcq, H., Dagorn, L., and Fonteneau, A.
695 2014. Spatial management of Indian Ocean tropical tuna fisheries: potential and
696 perspectives. ICES Journal of Marine Science 71: 1728–1749. doi:10.1093/icesjms/fst233
697 Koldewey, H. J., Curnick, D., Harding, S., Harrison, L. R., and Gollock, M. 2010. Potential benefits
698 to fisheries and biodiversity of the Chagos Archipelago/British Indian Ocean Territory as a
699 no-take marine reserve. Marine Pollution Bulletin 60: 1906–1915.
700 doi:10.1016/j.marpolbul.2010.10.002
701 Korneliussen, R. J., Heggelund, Y., Eliassen, I. K., Øye, O. K., Knutsen, T., and Dalen, J. (2009).
702 Combining multibeam-sonar and multifrequency-echosounder data: examples of the
703 analysis and imaging of large euphausiid schools. ICES Journal of Marine Science, 66(6),
704 991–997. http://doi.org/10.1093/icesjms/fsp092
705 Lan, K.-W., Evans, K., and Lee, M.-A. 2013. Effects of climate variability on the distribution and
706 fishing conditions of yellowfin tuna (*Thunnus albacares*) in the western Indian Ocean.
707 Climatic Change 119: 63–77. doi:10.1007/s10584-012-0637-8

708 Letessier, T. B., Meeuwig, J. J., Gollock, M., and others. 2013. Assessing pelagic fish populations:
709 The application of demersal video techniques to the mid-water environment. Methods in
710 Oceanography 8: 41–55. doi:10.1016/j.mio.2013.11.003
711 Letessier, T. B., Juhel, J.-B., Vigliola, L., and Meeuwig, J. J. 2015. Low-cost small action cameras
712 in stereo generate accurate measurements of fish. Journal of Experimental Marine Biology
713 and Ecology 466: 120–126. doi:10.1016/j.jembe.2015.02.013
714 Letessier, T. B., Cox, M. J. , Meeuwig, J. J., Boersch-Supan, P. H., and Brierley, A. S. 2016.
715 Enhanced pelagic biomass around coral atolls. Marine Ecology Progress Series. 546: 271–
716 276. doi:10.3354/meps11675
717 Letessier, T. B., Bouchet, P. B., and Meeuwig J. J. 2017. Sampling mobile oceanic fishes and
718 sharks: implications for fisheries and conservation planning. Biological reviews 92: 627–646.
719 Letessier, T. B., Mouillot, D., Bouchet, P. J., Vigliola, L., Fernandes, M. C., Thompson, C., and
720 others. (2019). Remote reefs and seamounts are the last refuges for marine predators
721 across the Indo-Pacific. PLoS Biology, 17(8), e3000366.
722 Maclennan, D. N., Fernandes, P. G., and Dalen, J. 2002. A consistent approach to definitions
723 and symbols in fisheries acoustics. ICES Journal of Marine Science 59: 365–369.
724 doi:10.1006/jmsc.2001.1158
725 MacNeil, M. A., Graham, N. A. J., Cinner, J. E. and others. 2015. Recovery potential of the
726 world's coral reef fishes. Nature 520: 341–344. doi:10.1038/nature14358
727 Madureira, L., Ward, P., and Atkinson, A. 1993. Differences in backscattering strength
728 determined at 120 and 38 kHz for three species of Antarctic macroplankton on JSTOR.
729 Marine Ecology Progress Series 93: 17–24.
730 Masumoto, Y., Horii, T., Ueki, I., Hase, H., Ando, K., and Mizuno K. 2008. Short-term upper-
731 ocean variability in the central equatorial Indian Ocean during 2006 Indian Ocean Dipole

event. Geophysical Research Letters 35: L14S09. doi:10.1029/2008GL033834@10.1002/(ISSN)1944-8007.MONSOON1

Maxwell, S. M., and Morgan, L. E. 2013. Foraging of seabirds on pelagic fishes: implications for management of pelagic marine protected areas. Marine Ecology Progress Series 481: 289–303.

Meeuwig, J. J., Thompson, C., Forrest, A., Jabour Christ, H., Letessier, T. B., and Meeuwig, D. J. (2021). Pulling Back the Blue Curtain: a Pelagic Monitoring Program for the Blue Belt. Frontiers in Marine Science.

Morais, R. A., and Bellwood, D. R. (2019). Pelagic Subsidies Underpin Fish Productivity on a Degraded Coral Reef. Current Biology, 1–26. http://doi.org/10.1016/j.cub.2019.03.044

Murphy, H. M., and Jenkins G. P. 2010. Observational methods used in marine spatial monitoring of fishes and associated habitats: a review. Marine Freshwater Research 61: 236–252. doi:10.1071/MF09068

Pacoureau, N., Rigby, C. L., Kyne, P. M., Sherley, R. B., Winker, H., Carlson, J. K., and others. (2021). Half a century of global decline in oceanic sharks and rays. *Nature*, 1–21. http://doi.org/10.1038/s41586-020-03173-9

Perez Correa, J., Carr, P., Meeuwig, J. J., Koldewey, H. J., and Letessier, T. B. (2020). Climate oscillation and the invasion of alien species influence the oceanic distribution of seabirds. Ecology and Evolution, 271(4), S246–19. http://doi.org/10.1002/ece3.6621

Pinheiro, J. C., and D. M. Bates. 2000. Mixed-Effects Models in S and S-PLUS.

Priede, I. G., and Merrett, N. R. 1996. Estimation of abundance of abyssal demersal fishes; a comparison of data from trawls and baited cameras. Journal of Fish Biology 49: 207–216. doi:10.1111/j.1095-8649.1996.tb06077.x

755 Proud, R., Cox, M. J., and Brierley, A. S. 2017. Biogeography of the Global Ocean's Mesopelagic
756 Zone. Current Biology 113–119. doi:10.1016/j.cub.2016.11.003
757 Proud, R., Handegard, N. O., Kloser, R. J., Cox, M. J., Brierley, A. S. Handling editor: David
758 Demer. 2018. From siphonophores to deep scattering layers: uncertainty ranges for the
759 estimation of global mesopelagic fish biomass. ICES Journal of Marince Science 3: 1.
760 doi:10.1121/1.421470
761 Rattle, J. 2019. A case study on the management of yellowfin tuna by the Indian Ocean Tuna
762 Commission. A Blue Marine Foundation report 1–23.
763 Resplandy, L., Vialard, J., Levy, M., Aumont, O., and Dandonneau Y. 2009. Seasonal and
764 intraseasonal biogeochemical variability in the thermocline ridge of the southern tropical
765 Indian Ocean. Journal of Geophysical Research 114: 1–13. doi:10.1029/2008JC005246
766 Rosen, S., Jørgensen, T., Hammersland-White, D., and Holst, J. C. 2013. DeepVision: a stereo
767 camera system provides highly accurate counts and lengths of fish passing inside a trawl.
768 Canadian Journal of Fisheries and Aquatic Science 70: 1456–1467. doi:10.1139/cjfas-2013-
769 0124
770 Sala, E., Lubchenco, J., Grorud-Colvert, K., Novelli, C., Roberts, C. and Sumaila, U. R. 2018.
771 Assessing real progress towards effective ocean protection. Marine Policy 91: 11–13.
772 doi:10.1016/j.marpol.2018.02.004
773 Sala, E., Mayorga, J., Bradley, D., Cabral, R. B., Atwood, T. B., Auber, A., and others (2021).
774 Protecting the global ocean for biodiversity, food and climate. Nature, 1–15.
775 http://doi.org/10.1038/s41586-021-03371-z
776 Santana-Garcon, J., Braccini, M., Langlois, T. J., Newman, S. J., McAuley, R., and Harvey E. S.
777 2014. Calibration of pelagic stereo-BRUVs and scientific longline surveys for sampling sharks.
778 Methods Ecology Evolution 824–833.

779 Santana-Garcon, J., Newman, S. J., Langlois, T. J., & Harvey, E. S. (2014). Effects of spatial closure
780 on highly mobile fish species: an assessment using pelagic stereo-BRUVS. Journal of
781 Experimental Marine Biology and Ecology, *460*(C), 153–161.
782 http://doi.org/10.1016/j.jembe.2014.07.003
783 Schobernd, Z. H., Bacheler, N.M., Conn, P.B., Trenkel, V. 2014. Examining the utility of alternative
784 video monitoring metrics for indexing reef fish abundance. Canadian Journal of Fisheries and
785 Aquatic Sciences 71:464–71.

786 Schott, F. A., and McCreary Jr. J. P. 2001. The monsoon circulation of the Indian Ocean. Progress
787 in Oceanography 51: 1–123.
788 Sheppard, C. R. C., Ateweberhan, M., Bowen, B. W. and others. 2012. Reefs and islands of the
789 Chagos Archipelago, Indian Ocean: why it is the world's largest no-take marine protected
790 area. Aquatic Conservation: Marine Freshwater Ecosystem 31: 232–261.
791 doi:10.1002/aqc.1248
792 Sherman, C. S., Chin, A., Heupel, M. R., and Simpfendorfer, C. A. 2018. Are we underestimating
793 elasmobranch abundances on baited remote underwater video systems (BRUVS) using
794 traditional metrics? Journal of Experimental Marine Biology and Ecology 503: 80–85.
795 doi:10.1016/j.jembe.2018.03.002
796 Sibert, J., Senina, I., Lehodey, P., and Hampton, J. 2012. Shifting from marine reserves to
797 maritime zoning for conservation of Pacific bigeye tuna (*Thunnus obesus*). Proceedings of
798 the National Academy of Sciences 109: 18221–18225. doi:10.1073/pnas.1209468109
799 Simmonds, E. J., and Maclennan, D. N. 2005. Fisheries acoustics: theory and practise, 2nd ed.
800 Chapman and Hall, London.

Surette, T., LeBlanc, C. H., Claytor, R. R., and Loots, C. 2015. Using inshore fishery acoustic data on Atlantic herring (*Clupea harengus*) spawning aggregations to derive annual stock abundance indices. Fisheries Research 164: 266–277. doi:10.1016/j.fishres.2014.12.010

Teng, M., Nathoo, F.S., Johnson, T.D. 2017. Bayesian Computation for Log-Gaussian Cox Processes: A Comparative Analysis of Methods. Journal of statistical computation and simulation 87:2227–52.

Watson, D. L., Harvey, E. S., Anderson, M. J., and Kendrick, G. A. 2005. A comparison of temperate reef fish assemblages recorded by three underwater stereo-video techniques. Marine Biology 148: 415–425. doi:10.1007/s00227-005-0090-6

Watkins, J. L., and Brierley, A. S. (2002). Verification of the acoustic techniques used to identify Antarctic krill. ICES Journal of Marine Science, *59*(6), 1326–1336.

Webber, B. G. M., Matthews, A. J., Heywood, K. J., and Stevens, D. P. 2012. Ocean Rossby waves as a triggering mechanism for primary Madden–Julian events. Quarterly Journal of the Royal Meteorological Society 138: 514–527. doi:10.1002/qj.936

Whitmarsh, S.K., Fairweather, P.G., Huveneers, C. 2016. What is Big BRUVver up to? Methods and uses of baited underwater video. Reviews in Fish Biology and Fisheries 27:53–73.

Wood, S. 2006. Generalized Additive Models: An introduction with R. 391.

Yates, K. L., Bouchet, P. J., Caley, M. J., and others. 2018. Outstanding Challenges in the Transferability of Ecological Models. Trends in ecology and evolution 33: 790–802. doi:10.1016/j.tree.2018.08.001

Yesson, C., Letessier, T. B., Nimmo-Smith, A., Hosegood, P., Brierley, A. S., Harouin, M., and Proud, R. (2020). Improved bathymetry leads to 4000 new seamount predictions in

theglobal ocean. UCL Open: Environment Preprint, 1–14.

http://doi.org/10.14324/111.444/000044.v1